Plug-flow does not exist in electro-osmosis

Rajib Chakraborty*

Department of Physical Sciences, Indian Institute of Science Education and Research (IISER) Kolkata, Mohanpur Campus, Mohanpur-741 252, West Bengal, India

(Dated: June 5, 2014)

Abstract

I eliminate hundred years old notion of 'plug-flow' in electro-osmosis, which was predicted by incomplete 'electric double layer' (EDL) theory. A recently developed 'electric triple layer' (ETL) theory removes some serious shortcomings of EDL theory regarding conservation of electric charge, and when applied to electro-osmosis, shows that the velocity profile is not 'plug-like' at all, but more like a parabola; it agrees with experiments and molecular dynamical simulation (MDS) results. Also, I redefine Helmholtz-Smoluchowski velocity-scale, which clears certain misunderstandings regarding representation of flow direction, and accommodates solution and geometrical properties within it. I describe some novel electro-osmotic flow controlling mechanisms. The entire electrokinetic theory must be modified using these concepts.

PACS numbers: 47.61.-k, 82.45.-h, 47.65.-d, 85.85.+j

* 89/3 Tanupukur Road, Dhakuria, Calcutta 700 031, West Bengal, India

; mecrajib@gmail.com

Electro-osmosis concerns flow of an electrolytic fluid relative to charged surfaces, driven by external electric field, and is a quite old field of study [1, 2]. It has important applications in different fields like micro-pumping micro-mixing, chemical separation and analysis etc. [3–7]. If a charged wall is exposed to an electrolytic solution, it attracts ions of opposite polarity (counter-ions) and repels ions of same polarity (co-ions), hence, spatial distribution of counter-ions and co-ions are not the same. As a result, an elemental fluid volume contains a net charge, and experience force in an external electric field. Hence, an axial field can drive the fluid through a channel made of charged walls.

It is obvious that a precise knowledge of charge-density (ρ_e) as a spatial function is very important in the study of electro-osmosis, because it appears in the body-force term of the fluid momentum equation that must be solved to get the velocity profile. A widely used expression for ρ_e comes from EDL theory [8, 9], and for extreme values of some parameters, it predicts that the velocity profile should appear like a 'plug', which is flat in most parts and hence it can be approximated that the fluid bulk moves as a whole with a finite slip with respect to wall. The myth of plug remains alive since hundred years, although there is no convincing experimental evidence in favor of it (to my knowledge). A recent development (see Ref [10]), it is pointed out that EDL theory has certain drawbacks, as it did not take care of charge conservation principle properly; consequently a novel ETL theory evolves that removes that discrepancy and an entirely different expression for ρ_e is obtained. In this paper I will discuss how the new distribution changes the form of velocity profile totally; it is not a plug at all, but tends to a parabola for some extreme conditions. Also there was another serious problem in the old expression for normalized velocity: it always appears positive, although a reversal of axial electric field must reverse the flow. I removed this problem here with a fine tuning of well-known Helmholtz-Smoluchowski velocity scale; a redefinition of the scale arises quite naturally that accommodates some solution and geometric properties.

I use the same rectangular geometry, axes convention and notations as in Ref [10], (also see [11]); however, I describe a few important symbols again. The channel, containing electrolytic solution, is of width $2a \ll$ length; y-axis is aligned with long, vertical channel-axis, x-axis is perpendicular to this. Long, charged walls are at $x = \pm a$. Unlike before, the narrow ends of the domain are open, allow fluid to enter or leave the domain. The fluid has uniform material properties: permittivity ϵ, viscosity μ etc. The x-distance is non-dimensionalized: $\eta \equiv x/a$. An important non-dimensional parameter is $\kappa \equiv a/\lambda_D$, where λ_D

is Debye length scale. The net charge in a cross-section of the domain is Q_0. Any expression with suffix 'Old' has a corrected version with suffix 'Corr'. A uniform external axial electric field E_y is used to drive the flow.

Since the domain is long and narrow, the flow may be assumed to be of low Reynolds number (that means non-linear terms in the fluid momentum equation can be neglected) and hydrodynamically fully developed (i.e. nothing varies along axial direction); the fluid momentum equation assumes very simple form [12]; only the axial velocity v is present, which varies only with x.

$$0 = \mu \frac{d^2 v}{dx^2} + \rho_e E_y \tag{1}$$

In order to solve the above equation for v, we must know ρ_e as a spatial function; below I write ρ_e as a function of η, derived from old EDL theory and corrected ETL theory respectively (see Ref [8, 10]).

$$\rho_{e,Old} = -\frac{\epsilon \kappa^2 \zeta}{a^2} \frac{\cosh(\kappa \eta)}{\cosh(\kappa)} \tag{2}$$

$$\rho_{e,Corr} = \left(\frac{\epsilon \kappa^2 \zeta}{a^2}\right) \left[\frac{\tanh(\kappa)}{\kappa} - \frac{\cosh(\kappa \eta)}{\cosh(\kappa)}\right] + \left(\frac{Q_0}{2}\right) \tag{3}$$

Where ζ arises from specifying electrostatic potential ψ at boundaries: $\psi|_{\eta=\pm 1} = \zeta$, see Refs. [8, 9]. Now, for $\kappa = 25$, I plot $\rho_{e,Old}$ in Fig. 1(a) and $\rho_{e,Corr}$ in Fig. 1(b); I use $Q_0 = 0$ for the later (see Ref [10] for details).

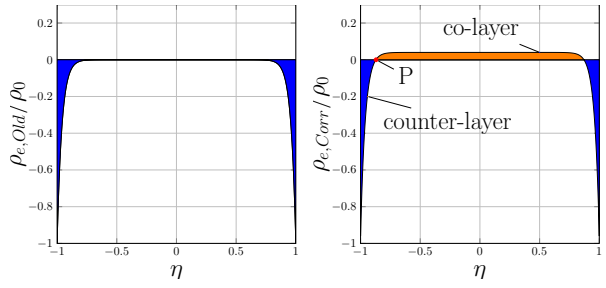

(a) (b)

FIG. 1. (Color online) Charge density distribution along channel cross-section, in an electrolytic solution, enclosed by *positively* charged walls. (a) In **EDL** theory, counter-ions dominate everywhere; incompatible with an electrically neutral (as a whole) solution. (b) In **ETL** theory; counter-layer and co-layer (i.e. counter-ion and co-ion dominated layer) form near and away from wall; their algebraic sum is the net charge Q_0 (=0, here); point 'P' is electrically neutral.

Using $\rho_{e,Old}$ in the momentum equation and solving it with no-slip boundary condition at walls (i.e. at $\eta = \pm 1$, $v = 0$), the velocity profile obtained (see [9, 13]) is given by, $v_{Old} = (\epsilon\zeta E_y/\mu)\,[\cosh(\kappa\eta)/\cosh(\kappa) - 1]$. When κ is large, v_{Old} asymptotically tends to $(-\epsilon\zeta E_y/\mu)$; that is perhaps the reason why most of the authors [5, 7, 8, 12, 14–16] defined a velocity scale called 'Helmholtz-Smoluchowski velocity scale', given by $v_{H.S.Old} \equiv -(\epsilon\zeta E_y/\mu)$, (please note the minus sign); it has the same direction as v_{Old} for all values of κ (since $|\eta| \leq 1 \Rightarrow \cosh(\kappa\eta) \leq \cosh(\kappa)$). The scaled velocity is given by,

$$\bar{v}_{Old} \equiv \frac{v_{Old}}{v_{H.S.Old}} = \left[1 - \frac{\cosh(\kappa\eta)}{\cosh(\kappa)}\right] \tag{4}$$

I plot $\bar{v}_{Old}$ vs η in Fig. 2(a), it always 'looks' $+ve$, for all sign-combinations of ζ and E_y, although, for a given ζ, the velocity should reverse in direction if E_y is reversed. So, the scale $v_{H.S.Old}$ caused lots of confusions and misunderstandings. Some authors [17, 18] tried to justify the minus sign in $v_{H.S.Old}$ by considering some particular sign combinations of ζ and E_y, that gives $+ve$ velocity (e.g. $-ve$ wall charge with $E_y > 0$), but remained silent about other combinations that should give $-ve$ velocity. A better scale could have been,

$$v_{H.S.Int} \equiv |(\epsilon\zeta E_y/\mu)| \tag{5}$$

The suffix 'Int' means 'Intermediate', that will be modified later. Using this I get,

$$\bar{v}_{Old,Int} \equiv \frac{v_{Old}}{v_{H.S.Int}} = sgn(\zeta E_y)\left[\frac{\cosh(\kappa\eta)}{\cosh(\kappa)} - 1\right] \tag{6}$$

$sgn(\zeta E_y)$ assumes value ± 1 when the sign of the product 'ζE_y' is $\pm ve$. When ζ and E_y are of the same sign, velocity is in $-ve$ y-direction, see Fig. 2(b). When ζ and E_y are of opposite sign, the direction reverses, see Fig. 2(c). The direction of $\bar{v}_{Old,Int}$ is consistent with $\rho_{e,Old}$; see Eq. 2 and Fig. 1(a). For $\zeta > 0$, old theory predicts the fluid to contain excess $-ve$ counter-ions every where, which experience negative force for $E_y > 0$ and hence fluid moves in negative direction. When electric field is reversed i.e. $E_y < 0$, the $-ve$ charges are forced in $+ve$ direction and fluid moves in that direction. Other sign-combinations of ζ and E_y can be explained similarly. Thus introduction of $v_{H.S.Int}$ removes discrepancies regarding flow direction, and is very important for checking whether the direction of flow predicted by theory is matching with experiment or not; the old scale was a source of confusion regarding this issue. Although the directional problem is corrected using $v_{H.S.Int}$, the velocity is still erroneous, for, it has been derived with erroneous EDL theory.

Now, I substitute $\rho_{e,Corr}$ (see Eq. 3) in the momentum equation (Eq. 1). Using boundary condition $v = 0$ at $\eta = 1$, and the fact that flow is symmetric about channel axis, the corrected velocity profile v_{Corr} is obtained. Now, a new velocity scale $v_{H.S.Corr}$ arises naturally and is given by,

$$v_{H.S.Corr} \equiv |\,(\epsilon\zeta E_y \kappa \tanh(\kappa)/\mu)\,| \tag{7}$$

The parameter κ may vary widely through different set of problems, which can change the characteristic velocity significantly. It happens, because, (see definition of λ_D in Ref. [10]) a change in solution concentration or temperature, affects the charge distribution; higher valency means higher electric force per ion; a wider channel (higher value of 'a') increases flow due to less friction etc. So, a velocity scale must contain $\kappa(\equiv a/\lambda_D)$. The corrected velocity scale accommodates κ that was absent in the older scale given by Eq. 5. One remark: if we add some salt (electrically neutral as a whole) to the solution, that increases the solution concentration and hence κ increases, but the net charge Q_0 does not change. This could not be handled with old theory: the net charge in the solution is given by $\int \rho_{e,Old}$ and a given value of κ fixes the net charge (see Eq. 2), and it changes when κ changes. The new theory can handle this very well, because κ and Q_0 are independent, so it is possible to vary κ while keeping Q_0 constant; it could be useful for adjusting flow-rate. The corrected normalized velocity, $\bar{v}_{Corr} \equiv (v_{Corr})/(v_{H.S.Corr})$ is given by,

$$\bar{v}_{Corr} = sgn(\zeta E_y)\left[\frac{1}{\kappa\tanh(\kappa)}\left(\frac{\cosh(\kappa\eta)}{\cosh(\kappa)} - 1\right) + \frac{(1+\sigma_0)}{2}\left(1-\eta^2\right)\right] \tag{8}$$

$$\text{Where,}\quad \sigma_0 = \frac{Q_0 a^2}{2\epsilon\zeta\kappa\tanh(\kappa)} \tag{9}$$

The first and the second term in the right hand side of Eq. 8 can be termed as 'hyperbolic' and 'parabolic' respectively; for small values of κ, both terms are significant, while, for large values of κ, the hyperbolic term tends to zero, and the profiles are parabolic. I plot $\bar{v}_{Corr}$ in Fig. 2(d) for $\kappa = 5$, and in Fig. 2(e) for $\kappa = 250$; the graphs are plotted with different values of σ_0, and with $sgn(\zeta E_y) = +1$; $\zeta > 0, E_y > 0$ in particular. For both cases, addition of co-ions (increasing σ_0) increases flow in positive direction (due to greater electric force in that direction), and addition of counter-ions (decreasing σ_0) tends to retard the flow (increases electric force in the opposite direction) as expected. For high value of $\kappa(= 250)$ the parabolic profiles are clearly seen in Fig. 2(e). Now, $\sigma_0 = -1$ needs special attention (for large κ), the profile tends to zero identically. Since the parabolic term in Eq. 8 vanishes,

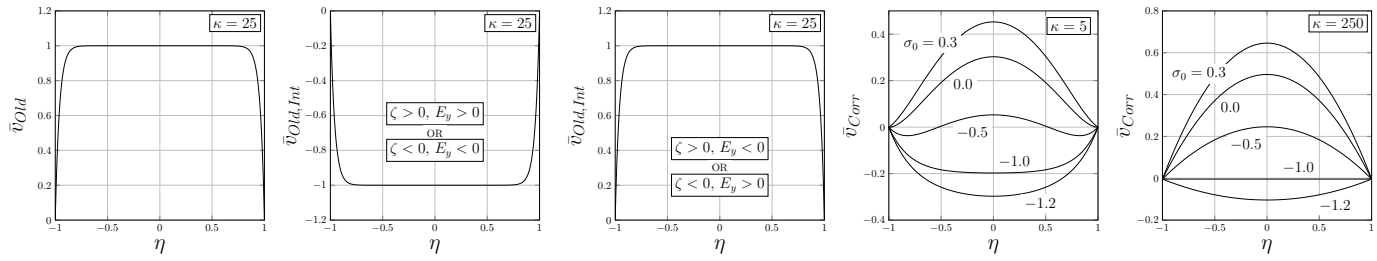

(a) (b) (c) (d) (e)

FIG. 2. Electro-osmotic velocity profiles (normalized) at different stages of correction. (a) $\bar{v}_{Old}$ is always $+ve$, indifferent of reversal of E_y; shape tends to 'plug-like' as κ increases (here, $\kappa = 25$). (b-c) $\bar{v}_{Old,Int}$ has same shape as $\bar{v}_{Old}$, but show reversal of flow when E_y is reversed for a given ζ. (d) $\bar{v}_{Corr}$ with small $\kappa(= 5)$, for different values of σ_0; shapes are not 'plug-like' at all; flow may not be unidirectional for some values of σ_0 e.g. -0.5. (e) $\bar{v}_{Corr}$ with large $\kappa(= 250)$, for different values of σ_0; shapes are parabolic in most parts in general; for $\sigma_0 = -1$, tends to identically zero. For both (d-e), $sgn(\zeta E_y) = +1$. For given E_y and ζ, the direction of $\bar{v}_{Corr}$ may change when σ_0 changes.

at a first glance it may appear that a plug is possible. However, it is impossible to make σ_0 exactly equal to -1 in experiments, and a very small deviation is sufficient to put both the parabolic and hyperbolic terms on equal footings, because the later itself is very small due to large value of κ (that it required for a plug). Hence, we never see plug in experiments.

If we change κ or/and σ_0, the spatial distributions of different types of ions change, which changes $+ve$ and $-ve$ electric forces on each elemental fluid volume. Hence, the velocity profile also changes to adjust the frictional force so that all kinds of forces add up to give zero axial force so that fluid velocity is constant in axial direction.

Differentiating Eq. 8 w.r.t η I get, $d\bar{v}_{Corr}/d\eta = sgn(\zeta E_y)\,[\sinh(\kappa\eta)/\sinh(\kappa) - (1 + \sigma_0)\eta]$. At $\eta = +1$,

$$(d\bar{v}_{Corr}/d\eta)|_{\eta=+1} = -\sigma_0 sgn(\zeta E_y) \tag{10}$$

Fig. 2(d) clearly demonstrates the meaning of the Eq. 10, here $sgn(\zeta E_y) = +1$, so, when $\sigma_0 > 0$ (say, 0.3) i.e. excess co-ions, the derivative at $\eta = +1$ is $-ve$, flow is unidirectional. When $\sigma_0 = 0$ i.e. when the solution is electrically neutral as a whole, the derivative is zero, the flow is still unidirectional. When there is some excess counter-ions i.e. $\sigma_0 <$

0, derivative becomes $+ve$, the flow starts to reverse near walls. Since counter-ions have more concentration near walls, increasing their number causes greater electric force in $-ve$ direction. However, for small $-ve$ values of σ_0 (say, -0.5), there are still many co-ions at the middle, and the positive electric force keeps fluid motion in positive direction there; we see, fluid moves in opposite directions in different parts of the same domain; some where in between the velocity is zero, it can be called 'stagnant line' (for 3-D domain there will be a 'stagnant plane' or a 'stagnant surface'). As counter ions increase in number, at some point the fluid starts moving entirely in the $-ve$ direction.

From Eq. 9 it can be seen that if Q_0 is not too large, for concentrated solution i.e. when κ is large (see definition of λ_D in Ref [10]), $\sigma_0 \ll 1$. So, for a concentrated solution, a little bit of excess charge does not affect the flow rate. However, for a dilute solution (small κ), flow rate can be considerably increased (decreased) by adding extra co-ions (counter-ions).

One remark: If fresh solution (electrically neutral as a whole) enters in the domain, it wipes out residual excess charge (if any) soon, and we can assume $Q_0 = 0$.

We see that the long standing notion of 'plug-like' velocity profile gets eliminated. In old EDL theory the fluid domain contained excess counter-ions every where (see Fig. 1(a)); for large values of κ, they are concentrated near the wall , thus the electrical force was also concentrated in a narrower region, creates a high shear, moves the fluid in that region and that drags the bulk fluid, so that the 'plug' formed (Fig. 2(a)). However, in the new ETL theory, an opposite electric force is active in the central part of the domain (on the co-layer, see Fig. 1(b)) and, for large κ, the resultant velocity profile is not flat 'plug-like', but 'parabolic' (Fig. 2(e)). The parabolic profile reminds us the flow driven by a constant axial pressure gradient (Poiseuille flow [9, 18]). High value of κ means a very narrow counter-layer; the co-layer is wide and of almost uniform amplitude. Hence, uniform axial electric field causes uniform axial body force in most part of domain, the solution has the same form when a constant pressure gradient drives the flow, and the profile is parabolic.

In Ref [19], authors reported an MDS result where fluid moves in opposite directions in different parts of the same domain, but in the old framework of charge distribution, it was not possible to explain the result, because, presence of excess counter-ions every where causes an unidirectional electric force under a uniform external electric filed and flow direction must be unidirectional as there is no other driving force; the authors say that the flow with smaller magnitude is a 'statistical noise'. However, presence of two layers

of opposite polarities according the ETL theory can explain that result very well, opposite driving force can cause the fluid to move in opposite directions under some special conditions (see Fig. 2(d)); presence of viscous forces does not allow it to take place 'always'. In Ref [20], the authors presented more MDS results that can be explained with the theory developed here.

In Ref [21, 22], the authors reported experimental fact: when axial electric field is increased, the velocity profile more clearly shows parabolic shape, that certainly cannot be explained with old theory. They studied flow inside cylindrical geometry, unlike in this paper (here 2-D rectangular domain is selected to convey the basic physics in the simplest possible manner). However, qualitative nature of flow must be similar for 2-D and 3-D, analogous to Poiseuille flow, which is parabolic both in 2-D rectangular and 3-D cylindrical domain. As I have discussed (see Eq. 8, and Fig. 2(d)), Fig. 2(e)), the shape may not be exactly parabolic, but in some cases resembles very closely to a parabola, especially for large values of κ. Increasing E_y increases $v_{H.S.Corr}$ (see Eq. 7) and hence the absolute velocity (which is actually observed in experiments) is scaled up everywhere by the same factor. In the axial part, the velocity is more, and so change in velocity becomes more than other parts, and it is easy to recognize the parabolic shape.

In summary, I corrected electro-osmotic velocity profile using **ETL** theory. For large values of parameter κ, the profile turned out to be 'parabolic' unlike a 'plug' that was predicted by old **EDL** theory; corrected profile has experimental and MDS supports. A natural redefinition of Helmholtz-Smoluchowski velocity scale arises; it captures flow reversal upon reversal of axial electric field. I discussed different flow controlling mechanisms, too.

I conclude by saying that the above analysis not only removes the 'myth' of plug-flow, but also opens up many other possibilities. Non-intuitive small-scale flow phenomena can be better explained and controlled with very simple analytical formulae. The presence of 'co-layer' in the **ETL** theory changed the entire scenario and a large volume of works in the entire field of electrokinetics must be modified using this concept.

I am grateful to Abhijit Sarkar, Sujata Sarkar, Fluent India, IIT Kharagpur, State Bank of India, IISER-Kolkata for direct/indirect funding for this work. Lessons on microfluidics from Suman Chakraborty and Ranabir Dey proved useful. Ananda Dasgupta's teaching about the indefiniteness of potential played key role here.

Appendix A: Derivation of corrected velocity profile

Using $\eta \equiv x/a$, the momentum equation reduces to,

$$\frac{d^2v}{d\eta^2} + \frac{\rho_e E_y a^2}{\mu} = 0 \tag{A1}$$

Rearranging terms in the expression for $\rho_{e,Corr}$, given by Eq. 3 (suppress suffix 'Corr'),

$$\begin{aligned}\rho_e &= \left(\frac{\epsilon\kappa^2\zeta}{a^2}\right)\left[\left(\frac{\tanh(\kappa)}{\kappa} + \frac{Q_0 a^2}{2\epsilon\kappa^2\zeta}\right) - \frac{\cosh(\kappa\eta)}{\cosh(\kappa)}\right] \\ &= \left(\frac{\epsilon\kappa^2\zeta}{a^2}\right)\left[N - \frac{\cosh(\kappa\eta)}{\cosh(\kappa)}\right]\end{aligned} \tag{A2}$$

$$\begin{aligned}\text{Where, } N &\equiv \left(\frac{\tanh(\kappa)}{\kappa} + \frac{Q_0 a^2}{2\epsilon\kappa^2\zeta}\right) \\ &= \frac{\tanh(\kappa)}{\kappa}\left(1 + \frac{Q_0 a^2}{2\epsilon\zeta\kappa\tanh(\kappa)}\right) \\ &= \frac{\tanh(\kappa)}{\kappa}(1+\sigma_0)\end{aligned} \tag{A3}$$

$$\text{Where, } \sigma_0 \equiv \frac{Q_0 a^2}{2\epsilon\zeta\kappa\tanh(\kappa)} \tag{A4}$$

Substituting ρ_e from Eq. A2 in Eq. A1 gives,

$$\begin{aligned}\frac{d^2v}{d\eta^2} + \left(\frac{E_y a^2}{\mu}\right)\left(\frac{\epsilon\kappa^2\zeta}{a^2}\right)\left[N - \frac{\cosh(\kappa\eta)}{\cosh(\kappa)}\right] &= 0 \\ \Rightarrow \frac{d^2v}{d\eta^2} + M\left[N - \frac{\cosh(\kappa\eta)}{\cosh(\kappa)}\right] &= 0\end{aligned} \tag{A5}$$

$$\text{Where, } M \equiv \left(\frac{E_y a^2}{\mu}\right)\left(\frac{\epsilon\kappa^2\zeta}{a^2}\right) = \left(\frac{\epsilon\kappa^2\zeta E_y}{\mu}\right) \tag{A6}$$

Integrating Eq. A5 twice w.r.t η,

$$v + MN\frac{\eta^2}{2} - \frac{M\cosh(\kappa\eta)}{\kappa^2\cosh(\kappa)} + C_1\eta + C_2 = 0 \tag{A7}$$

C_1 and C_2 are arbitrary constants. Symmetry about channel axis implies v is an even function of η, hence $C_1 = 0$. Also, at $\eta = 1$, $v = 0$ (no slip). Hence,

$$v + MN\frac{\eta^2}{2} - \frac{M\cosh(\kappa\eta)}{\kappa^2\cosh(\kappa)} + C_2 = 0 \tag{A8}$$

$$\frac{MN}{2} - \frac{M}{\kappa^2} + C_2 = 0 \tag{A9}$$

Substract Eq. A9 from Eq. A8, and group similar terms,

$$v = \frac{M}{\kappa^2}\left(\frac{\cosh(\kappa\eta)}{\cosh(\kappa)} - 1\right) + MN\frac{1}{2}\left(1 - \eta^2\right)$$

Using Eq. A3,

$$v = \frac{M}{\kappa^2}\left[\left(\frac{\cosh(\kappa\eta)}{\cosh(\kappa)} - 1\right) + \kappa\tanh(\kappa)\frac{(1+\sigma_0)}{2}\left(1-\eta^2\right)\right]$$
$$= \frac{M\kappa\tanh(\kappa)}{\kappa^2}\left[\frac{1}{\kappa\tanh(\kappa)}\left(\frac{\cosh(\kappa\eta)}{\cosh(\kappa)} - 1\right) + \frac{(1+\sigma_0)}{2}\left(1-\eta^2\right)\right] \tag{A10}$$

Define a new velocity scale (use Eq. A6),

$$v_{H.S.Corr} \equiv \left|\frac{M\kappa\tanh(\kappa)}{\kappa^2}\right| = \left|\frac{\epsilon\zeta E_y \kappa\tanh(\kappa)}{\mu}\right| \tag{A11}$$

Using Eq. A10 and Eq. A11, with suffix 'Corr' in v,

$$\bar{v}_{Corr} \equiv \frac{v_{Corr}}{v_{H.S.Corr}} \tag{A12}$$
$$= sgn(\zeta E_y)\left[\frac{1}{\kappa\tanh(\kappa)}\left(\frac{\cosh(\kappa\eta)}{\cosh(\kappa)} - 1\right) + \frac{(1+\sigma_0)}{2}\left(1-\eta^2\right)\right] \tag{A13}$$

---

[1] J. Lyklema, Colloids and Surfaces A: Physicochem. Eng. Aspects **222**, 5 (2003).

[2] S. Wall, Current Opinion in Colloid & Interface Sci. **15**, 119 (2010).

[3] N.-T. Nguyen and S. T. Wereley, *Fundamentals and Applications of Microfluidics* (Artech House, 685 Canton Street, Norwood, MA 02062, 2002).

[4] H. Stone, A. Stroock, and A. Ajdari, **36**, 381 (2004).

[5] S. Ghosal, **38**, 309 (2006).

[6] T. M. Squires and S. R. Quake, Rev. Mod. Phys. **77**, 977 (2005).

[7] R. B. Schoch, J. Han, and P. Renaud, Rev. Mod. Phys. **80**, 839 (2008).

[8] S. Chakraborty and D. Paul, Journal of Physics D: Applied Physics **39**, 5364 (2006).

[9] H. Bruus, *Theoretical Microfluidics* (Oxford University Press Inc., New York, United States, 2008).

[10] R. Chakraborty, "Electric triple layer theory," e-print viXra:1405.0354 (2014).

[11] Actually this 2-D domain represents cross-section of a 3-D geometry (except near boundaries in the third direction), when the domain extent in the third direction is very large.

[12] S. S. Dukhin, Advances in Colloid and Interface Science **35**, 173 (1991).

[13] R. Dey, D. Chakraborty, and S. Chakraborty, Journal of Heat Transfer **133**, 024503 (2011).

[14] M. Z. Bazant and T. M. Squires, Phys. Rev. Lett. **92**, 066101(4) (2004).

[15] A. Delgado, F. Gonzalez-Caballero, R. Hunter, L. Koopal, and J. Lyklema, J. Colloid & Interface Sci. **309**, 194 (2007).

[16] C. Zhao and C. Yang, Microfluid Nanofluid (2012), 10.1007/s10404-012-0971-1.

[17] R. J. Hunter, *Zeta Potential in Colloid Science: Principles and Applications* (Academic Press, 1981).

[18] J. Lyklema, *Fundamentals of Interface and Colloid Science,*, Vol. 2 (Academic, London, 1991).

[19] R. Qiao and N. R. Aluru, J. Chem. Phys. **118**, 4692 (2003).

[20] R. Qiao and N. R. Aluru, Phys. Rev. Lett. **92**, 198301(4) (2004).

[21] P. M. S. John, T. Woudenberg, C. Connell, M. Deshpande, J. R. Gilbert, M. Garguilo, P. Paul, J. Molho, A. E. Herr, T. W. Kenny, and M. G. Mungal, in *Proc. 8th IEEE Solid-State Sensor and Actuator Work-shop*, Hilton Head, SC (1998) pp. 106–111, held in June 7-11.

[22] J. I. Molho, A. E. Herr, M. Deshpande, J. R. Gilbert, M. Garguilo, P. M. S. J. P. Paul, T. M. Woudenberg, and C. Connell, in *Proc. ASME (MEMS)*, 66 (1998) pp. 69–76.